

# Unravelling the Di- and Oligomerisation Interfaces of the G-Protein Coupled Bile Acid Receptor TGR5 via Integrative Modelling

C. G. W. Gertzen, V. Keitel, C. A. M. Seidel, H. Gohlke

published in

## **NIC Symposium 2018**

K. Binder, M. Müller, A. Trautmann (Editors)

Forschungszentrum Jülich GmbH,  
John von Neumann Institute for Computing (NIC),  
Schriften des Forschungszentrums Jülich, NIC Series, Vol. 49,  
ISBN 978-3-95806-285-6, pp. 25.  
<http://hdl.handle.net/2128/17544>

© 2018 by Forschungszentrum Jülich

Permission to make digital or hard copies of portions of this work for personal or classroom use is granted provided that the copies are not made or distributed for profit or commercial advantage and that copies bear this notice and the full citation on the first page. To copy otherwise requires prior specific permission by the publisher mentioned above.

# Unravelling the Di- and Oligomerisation Interfaces of the G-Protein Coupled Bile Acid Receptor TGR5 via Integrative Modelling

Christoph G. W. Gertzen<sup>1,2</sup>, Verena Keitel<sup>1</sup>, Claus A. M. Seidel<sup>3</sup>, and Holger Gohlke<sup>2,4</sup>

<sup>1</sup> Clinic for Gastroenterology, Hepatology and Infectious Diseases, Heinrich Heine University Düsseldorf, 40225 Düsseldorf, Germany

<sup>2</sup> Institute for Pharmaceutical and Medicinal Chemistry, Heinrich Heine University Düsseldorf, 40225 Düsseldorf, Germany

<sup>3</sup> Chair for Molecular Physical Chemistry, Heinrich Heine University Düsseldorf, 40225 Düsseldorf, Germany

<sup>4</sup> John von Neumann Institute for Computing (NIC), Jülich Supercomputing Centre (JSC) and Institute for Complex Systems - Structural Biochemistry (ICS-6), Forschungszentrum Jülich, 52425 Jülich, Germany  
*E-mail: h.gohlke@fz-juelich.de*

TGR5 is a bile acid- and neurosteroid-sensing G-protein coupled receptor (GPCR), which is almost ubiquitously expressed throughout the human body. Its physiological functions comprise the regulation of blood glucose homeostasis, metabolism, and inflammation. Additionally, recent studies show an involvement of TGR5 in the formation of gastric, esophageal, and cholangiocyte cancers as well as in bile acid-induced itch. Hence, TGR5 has been identified as an important drug target. To reduce side effects of drugs targeting GPCRs, the development of bivalent ligands specifically targeting dimers was shown to be promising. To do so, the knowledge of the dimerisation interfaces of these GPCRs is paramount. However, the dimerisation interfaces of TGR5 are not known. Here, we present the identification of the primary dimerisation interface of TGR5 and possible oligomerisation interfaces. We used Multiparameter Image Fluorescence Spectroscopy (MFIS) Förster Resonance Energy Transfer (FRET) measurements of fluorescently labelled TGR5 in live cells to measure apparent distances between two TGR5 protomers and compared them to distances computed for putative TGR5 dimer models. As the linker between TGR5 and the fluorophores contained more than 30 residues, we used all-atom molecular dynamics (MD) simulations to sample the conformational space of the linker and fluorophore in relation to TGR5. The sampled configurations were reweighted by free energy calculations using the molecular mechanics Poisson-Boltzmann surface area (MM-PBSA) method to account for the presence of solvent and a membrane, and a random energy model to estimate the configurational entropy. This allowed us to identify the 1-8 interface of TGR5 as the primary dimerisation interface, with the 4-5 and 5-6 interfaces as possible oligomerisation sites. This information might be used to develop novel TGR5 ligands with a reduced side-effect profile.

## 1 Introduction

The Tanaka G-protein coupled receptor 5 (TGR5) is the first identified bile acid sensing GPCR<sup>1,2</sup>. While nearly ubiquitously expressed throughout the body, TGR5 is found in high expression levels in the intestine, the bile duct, the brain, and immunocompetent cells<sup>3</sup>. Being activated by hydrophobic bile acids and neurosteroids such as estradiol, TGR5 reg-

ulates blood glucose homeostasis, metabolism, and inflammatory response<sup>4</sup>. While activated TGR5 leads to proliferative and anti-apoptotic effects, overexpression of TGR5 can lead to the formation of bile duct cancer<sup>5</sup> or gastric and esophageal cancers<sup>6</sup>. Hence, the development of TGR5 antagonists with a narrow side effect spectrum is critical to devise a specific cure for these cancers. Recently, the development of bivalent GPCR ligands has been shown to be particularly promising with respect to reduced side effect<sup>7</sup>; such ligands target GPCR dimers. However, for TGR5, no structural information regarding dimerisation or higher oligomerisation has become available. Co-immunoprecipitation experiments performed by us showed that TGR5 wild type (WT) forms at least dimers<sup>15</sup>. Notably, a naturally occurring Y111A mutant showed 60% less dimerisation in co-immunoprecipitation assays than TGR5 WT. Here, we thus set out to construct structural models of the dimer and oligomeric TGR5 by combining Multiparameter Image Fluorescence Spectroscopy (MFIS) for quantitative Förster resonance energy transfer (FRET) analysis in live cells and integrative modelling<sup>15</sup>.

## 2 Methods

Dimer models of TGR5 based on known dimerisation interfaces from GPCR X-ray crystal structures were the starting point for the integrative modelling. These interfaces utilise transmembrane helix (TM) 1 and helix 8 (1-8 interface), TM 4 and 5 (4-5 interface), and TM 5 and 6 (5-6 interface) (Fig. 1).

To discriminate between the models, the fluorescent probes GFP and mCherry were fused to the C-terminus of TGR5 via a linker of 42 residues length. Then, MFIS FRET was used to measure the distribution of the apparent distances between the fluorophores in live cells. The apparent distances strongly depend on the distance between the C-termini of TGR5 and, thus, the respective TGR5 dimer model (see Fig. 1). Hence, one can discriminate between the TGR5 dimer models by computing distance distributions of the fluorescent probes attached to TGR5 and comparing those to the measured apparent distance distributions.

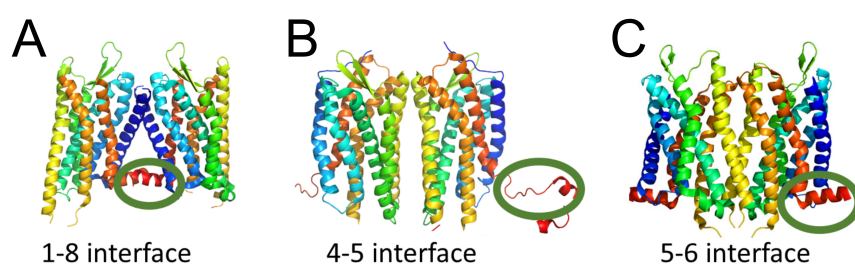


Figure 1. TGR5 dimer models based on X-ray crystal structures of GPCR dimers with different interfaces: **A** 1-8 interface as found in the  $\kappa$ -opioid receptor; **B** 4-5 interface as found in the CXCR4 receptor; **C** 5-6 interface as found in the  $\mu$ -opioid receptor. TGR5 monomer chains are rainbow-coloured starting with TM1 in blue to H8 in red. The C-terminus is indicated by an olive ellipse.

To perform the computation of the distance distributions of the fluorescent probes in an efficient manner, we pursued a step-wise strategy. Initially, for computing a thermodynamic ensemble (TE) of GFP positions with an explicit linker/GFP construct, the structure of the TGR5 C-terminal residues 296-330, for which no experimental structural information is available, and the nine residues that connect the C-terminus to GFP (total sequence: QRCLQGLWGRASRDSPGPSIAYHPSSQSSVDLDLNYGSTGRHVS) was generated in a straight peptide conformation, such that a structurally unbiased starting structure for the subsequent molecular dynamics (MD) simulations was obtained. This linker was subsequently fused to GFP (PDB ID: 4EUL<sup>8</sup>), and the resulting structure was capped with acetyl and *N*-methyl amide groups at the N- and C-termini, respectively, and protonated according to pH 7.4. We assumed the thermodynamic ensemble (TE) of mCherry to be identical to that of GFP.

Next, the linker/GFP construct was neutralised by adding counter ions and solvated in an octahedral box of TIP3P water<sup>9</sup> with a minimal water shell of 12 Å around the solute. The Amber14 package of molecular simulation software<sup>10,11</sup> and the ff14SB and GAFF<sup>12</sup> force fields were used to perform all-atom MD simulations. The first linker residue was fixed with positional harmonic restraints throughout the simulations to emulate that this residue would be bound to TGR5 embedded in a membrane. After energy minimisation and thermalisation to a pressure of 1 atm and a temperature of 300 K, six independent production runs of NVT-MD simulations with 150 ns length each were performed on JU-RECA. The conformations obtained in these simulations were pooled for further analyses.

Finally, we combined the snapshots of the simulations with the TGR5 dimer models

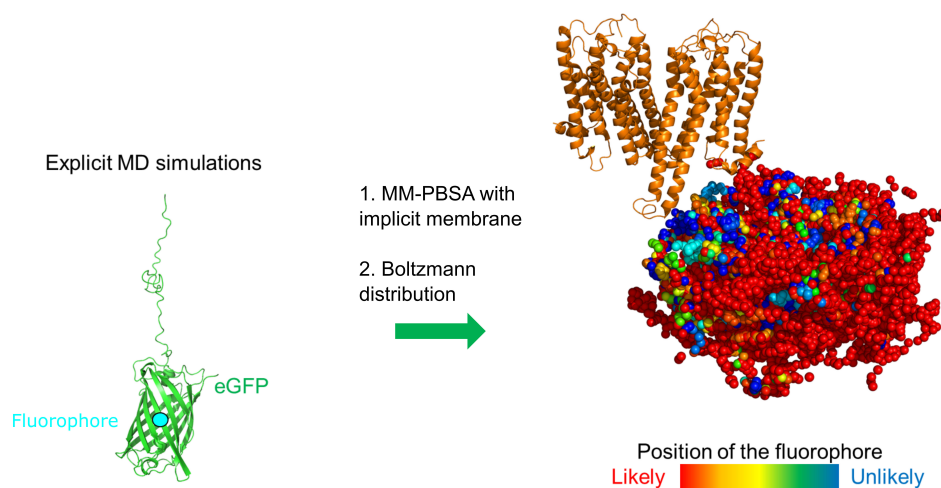


Figure 2. Schematic of the procedure to generate a TE of the linker/GFP construct. First, explicit all-atom MD simulations of the linker and fluorophore were conducted. Then, the conformations were combined with dimer models of TGR5 (Fig. 1) to calculate the conformational free energy via implicit membrane MM-PBSA calculations. Subsequently, these energies were corrected for the configurational entropy, and the result used to Boltzmann-weight the linker/GFP configurations with respect to the likelihood of the location of the fluorophore (dots on the right).

and calculated, first, effective energies of linker/GFP conformations in the presence of TGR5 dimers and an implicit membrane using the MM-PBSA approach<sup>13</sup>; for the membrane, a three-layer model with dielectric constants of 34, 4, and 1 for the outer to inner membrane slabs with a width of 5, 6, and 6 Å, respectively, was used. Those snapshots in which GFP penetrated the membrane, or in which GFP or the linker clashed with the TGR5 dimer, were omitted. The remaining snapshots showed that GFP essentially moves within a hemisphere on the cytosolic side of the membrane beneath the dimer (Fig. 2). For weighting the snapshots according to a Boltzmann distribution, second, the configurational entropy of the linker/GFP configurations needs to be considered. Here, we assumed that the entropy is dominated by the configurations of the linker, whereas configurations of GFP were assumed to provide no contribution. We considered the linker a random heteropolymer for which low energy conformations can structurally vary largely; therefore, a random energy model was used to describe its energy landscape and to compute its configurational entropy<sup>14</sup>. From the effective energy and configurational entropy, the weights of the locations of the GFP fluorophore were computed, and these weights were used to assign weights of the distances between the donor and acceptor fluorophores (Fig. 2).

### 3 Results

FRET between TGR5 molecules C-terminally fused to enhanced GFP as a donor or mCherry as an acceptor was measured for two different TGR5 variants: TGR5 WT and the Y111A variant. Both variants were shown to be fully functional by a cell-based assay.

FRET was detected in all TGR5 variants, indicating at least homodimerisation. Interestingly, the TGR5 variants showed differences in their FRET properties: Upon titration of the acceptor, the energy transfer efficiency did not change significantly in Y111A, in contrast to the WT. This indicates that the Y111A variant forms high amounts of dimers but not oligomers, as fluorescence quenching cannot occur in monomers, while the efficiency changes in the WT suggest that higher-order oligomers, at least tetramers, are present.

To quantify this, we formally described the fluorescence decays by two FRET rate constants, which are for convenience given in units of apparent distances  $R_{DA,app}$ . For all TGR5 variants, this rate constant fit resulted in a short apparent distance  $R_{DA,app-1}$  (high FRET) with a small fraction and a long apparent distance  $R_{DA,app-2}$  (low FRET) with a large fraction. In TGR5 WT, both apparent distances  $R_{DA,app-1}$  and  $R_{DA,app-2}$  became shorter ( $R_{DA,app-1} = 40\text{-}20$  Å;  $R_{DA,app-2} = 75\text{-}50$  Å) with increasing acceptor concentration. Furthermore, the species fractions also changed: The short distance-fraction increased from 7% to 30% in an acceptor-dependent manner, leading at the same time to a strong reduction of the long distance-fraction from 39% to 12%. This change is only possible if TGR5 WT exists as oligomers, because FRET cannot occur between distant, i.e., not oligomerised, dimers. While FRET is present in the Y111A variant, showing the formation of dimers, no concentration-dependence of the FRET fractions was found for the Y111A variant, showing that the Y111A variant only forms dimers but not higher-order oligomers.

These results were used to determine the di- and oligomerisation interfaces of TGR5. For this, the experimental  $R_{DA,app}$  was correlated to the computed  $R_{DA,app}$  (Fig. 3A) for dimer models of TGR5 (Fig. 1) and the respective TE of the fluorophore probes (Fig. 2). The experimental  $R_{DA,app}$  of the Y111A variant was used, as the titration experiments

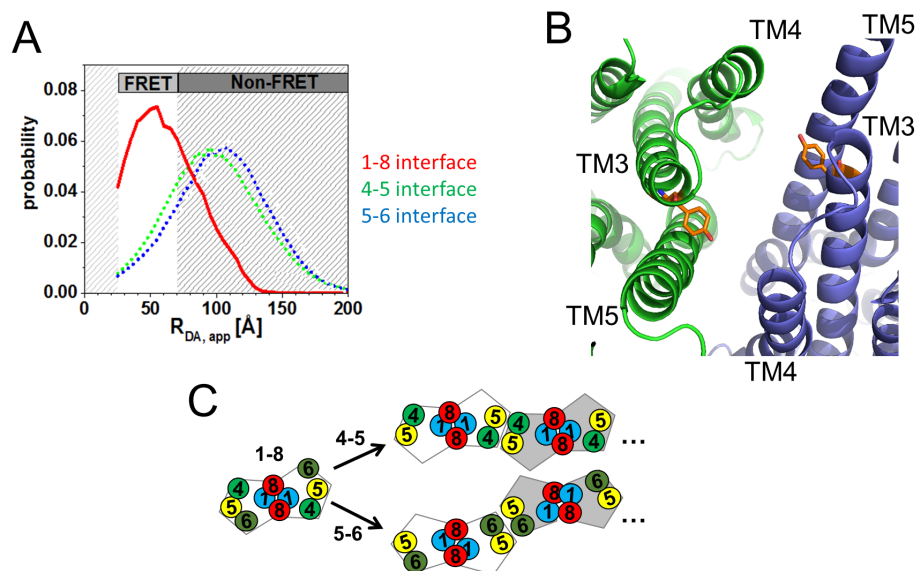


Figure 3. **A** Computed  $R_{DA,app}$  for dimer models of TGR5. The distributions show that FRET can only occur if the 1-8 interface is formed, without influence from other interfaces. **B** Influence of the Y111A mutation on oligomerisation. The TGR5 dimer model of the 4-5 interface is displayed as a cartoon viewed from the cytoplasm with one protomer coloured in green and one in navy. Residue Y111 located in TM3 is depicted in orange stick representation in each TGR5 monomer. **C** Possible oligomerisation states with 1-8 as the primary dimerisation interface, forming higher order dimers of dimers via either the 4-5 or the 5-6 interface. Figure was adapted from Ref. 15, published under a Creative Commons CC BY license.

suggested predominant homodimer formation of this variant. The computed  $R_{DA,app}$  for the 1-8 interface of TGR5 showed a remarkable similarity with the experimental  $R_{DA,app}$  of the Y111A variant Fig. 3A. Thus, the primary site for TGR5 homodimerisation is the 1-8 interface (Fig. 1A).

For the TGR5 WT, the titration experiments strongly suggested formation of dimers and higher-order oligomers, with the latter formed as oligomers of dimers. This finding implies the presence of at least a second interface for TGR5 oligomer formation, which involves Y111 (as the Y111A mutation abrogated oligomer formation). As shown in Fig. 3B, the Y111 residue located in TM3 can interact with TM5 or/and TM6 of another TGR5 molecule depending on its structural environment, which could be either helical or a flexible loop. Hence, both the 4-5 and 5-6 interfaces (Fig. 1B, C) could be potential interaction sites for oligomerisation. This leads to the suggestion that the TGR5 oligomers must resemble a one-dimensional array, with alternating 1-8 dimerisation and 4-5, or 5-6, oligomerisation interfaces (Fig. 3C).

## 4 Conclusion

We showed that TGR5 WT forms homo-oligomers. Thereby, dimerisation involves an interface formed by TM1 and helix 8, and oligomerisation additionally involves TM5. Obtaining these results was only possible by tightly integrating advanced MFIS-FRET experiments in live cells with comprehensive computations of the TE of fluorophore locations. Our results might aid in the development of novel TGR5 ligands with reduced side-effects.

## Acknowledgements

This work was supported by the Deutsche Forschungsgemeinschaft through the Collaborative Research Center SFB 974 (“Communication and Systems Relevance during Liver Damage and Regeneration”, Düsseldorf) and INST 208/704-1 FUGG (to H. G.) to purchase the hybrid compute cluster used in this study. We are grateful for the computing time provided by the John von Neumann Institute for Computing (NIC) to H. G. on the supercomputer JURECA (Project ID: HDD15) at Jülich Supercomputing Centre (JSC).

## References

1. Y. Kawamata, R. Fujii, M. Hosoya, M. Harada, H. Yoshida, M. Miwa, S. Fukusumi, Y. Habata, T. Itoh, Y. Shintani, S. Hinuma, Y. Fujisawa, and M. Fujino, *A G Protein-coupled Receptor Responsive to Bile Acids*, *Journal of Biological Chemistry* **278**, 9435–9440, 2003.
2. T. Maruyama, K. Tanaka, J. Suzuki, H. Miyoshi, N. Harada, T. Nakamura, Y. Miyamoto, A. Kanatani, and Y. Tamai, *Targeted disruption of G protein-coupled bile acid receptor 1 (Gpbar1/M-Bar) in mice*, *Journal of Endocrinology* **191**, 197–205, 2006.
3. V. Keitel, R. Reinehr, P. Gatsios, C. Rupprecht, B. Görg, O. Selbach, D. Häussinger, and R. Kubitz, *The G-protein coupled bile salt receptor TGR5 is expressed in liver sinusoidal endothelial cells*, *Hepatology* **45**, 695–704, 2007.
4. V. Keitel and D. Häussinger, *Perspective: TGR5 (Gpbar-1) in liver physiology and disease*, *Clinics and Research in Hepatology and Gastroenterology* **36**, 412–419, 2012.
5. V. Keitel, R. Reinehr, M. Reich, A. Sommerfeld, K. Cupisti, W. T. Knoefel, and D. Häussinger, *TGR5 (Gpbar-1) is expressed in cholangiocarcinomas and confers apoptosis resistance in isolated cholangiocytes*, *Z Gastroenterol* **50**, P5.24, 2012.
6. J. Hong, J. Behar, J. Wands, M. Resnick, L. J. Wang, R. A. DeLellis, D. Lambeth, R. F. Souza, S. J. Spechler, and W. Cao, *Role of a novel bile acid receptor TGR5 in the development of oesophageal adenocarcinoma*, *Gut* **59**, 170–180, 2010.
7. C. Hiller, J. Kühhorn, and P. Gmeiner, *Class A G-protein-coupled receptor (GPCR) dimers and bivalent ligands*, *Journal of Medicinal Chemistry* **56**, 6542–6559, 2013.
8. J. A. J. Arpino, P. J. Rizkallah, and D. Dafydd, *Crystal Structure of Enhanced Green Fluorescent Protein to 1.35 angstrom Resolution Reveals Alternative Conformations for Glu222*, *Plos One* **7**, e47132, 2012.

9. W. Jorgensen, J. Chandrasekhar, J. D. Madura, R. Impey, and M. L. Klein, *Comparison of simple potential functions for simulating liquid water*, The Journal of Chemical Physics **79**, 2, 1983.
10. D. A. Case, T. E. Cheatham, T. Darden, H. Gohlke, R. Luo, K. M. Merz, A. Onufriev, C. Simmerling, B. Wang, R. J. Woods, *The Amber biomolecular simulation programs*, Journal of Computational Chemistry **26**, 1668–1688, 2005.
11. D. A. Case, V. Babin, J. T. Berryman, R. M. Betz, Q. Cai, D. S. Cerutti, T. E. Cheatham III, T. A. Darden, R. E. Duke, H. Gohlke, A. W. Goetz, S. Gusarov, N. Homeyer, P. Janowski, J. Kaus, I. Kolossváry, A. Kovalenko, T. S. Lee, S. LeGrand, T. Luchko, R. Luo, B. Madej, K. M. Merz, F. Paesani, D. R. Roe, A. Roitberg, C. Sagui, R. Salomon-Ferrer, G. Seabra, C. L. Simmerling, W. Smith, J. Swails, R. C. Walker, J. Wang, R. M. Wolf, X. Wu and P. A. Kollman, *AMBER 14*, 2014.
12. J. M. Wang, R. M. Wolf, J. W. Caldwell, P. A. Kollman, and D. A. Case, *Development and testing of a general amber force field*, Journal of Computational Chemistry **25**, 1157–1174, 2004.
13. N. Homeyer and H. Gohlke, *Extension of the free energy workflow FEW towards implicit solvent/implicit membrane MM–PBSA calculations*, Biochimica et Biophysica Acta (BBA) - General Subjects **1850**, 972–982, 2015.
14. D. Wales, *Energy landscapes: Applications to clusters, biomolecules and glasses*, Cambridge University Press, 0521814154, 2003.
15. A. Greife, S. Felekyan, Q. Ma, C. G. W. Gertzen, L. Spomer, M. Dimura, T. O. Peulen, C. Wöhler, D. Häussinger, H. Gohlke, V. Keitel, and C. A. M. Seidel, *Structural assemblies of the di- and oligomeric G-protein coupled receptor TGR5 in live cells: an MFIS-FRET and integrative modelling study*, Scientific Reports **6**, 36792, 2016.